

Exact Conservation Laws of the Gradient Expanded Kadanoff–Baym Equations

J. Knoll¹, Yu. B. Ivanov^{1,2} and D. N. Voskresensky^{1,3}

¹*Gesellschaft für Schwerionenforschung mbH, Planckstr. 1, 64291
Darmstadt, Germany*

²*Kurchatov Institute, Kurchatov sq. 1, Moscow 123182, Russia*

³*Moscow Institute for Physics and Engineering, Kashirskoe sh. 31,
Moscow 115409, Russia*

E-mail: J.Knoll@gsi.de, Y.Ivanov@gsi.de, D.Voskresensky@gsi.de

It is shown that the Kadanoff–Baym equations at consistent first-order gradient approximation reveal exact rather than approximate conservation laws related to global symmetries of the system. The conserved currents and energy–momentum tensor coincide with corresponding Noether quantities in the local approximation. These exact conservations are valid, provided a Φ derivable approximation is used to describe the system, and possible memory effects in the collision term are also consistently evaluated up to first-order gradients.

1. INTRODUCTION

Non-equilibrium Green function techniques, developed by Schwinger, Kadanoff, Baym and Keldysh [1–4], provide the appropriate concepts to study the space–time evolution of many-particle quantum systems. This formalism finds now applications in various fields, such as quantum chromodynamics [5,6], nuclear physics, in particular heavy ion collisions [7–23], astrophysics [11,24,25], cosmology [26], spin systems [27], lasers [28], physics of plasma [29,30], physics of liquid ³He [31], critical phenomena, quenched random systems and disordered systems [32], normal metals and superconductors [24,33,34], semiconductors [35], tunneling and secondary emission [36], etc.

For actual calculations certain approximation steps are necessary. In many cases perturbative approaches are insufficient, like for systems with strong couplings as treated in nuclear physics. In such cases, one has to resum certain sub-series of diagrams in order to obtain a reasonable approximation scheme. In contrast to perturbation theory, for such resummations

one frequently encounters the fact that the scheme may no longer be conserving, although for each diagram considered the conservation laws are implemented at each vertex. Thus, the resulting equations of motion may no longer comply with the conservation laws, e.g., of currents, energy and momentum. This is a problem of particular importance for recent studies of particles with broad damping width such as resonances [18]. The problem of conservation laws in such resummation schemes has first been considered in two pioneering papers by Baym and Kadanoff [37, 38] discussing the response to an external perturbation of quantum systems in thermodynamic equilibrium. Baym, in particular, showed [38] that any approximation, in order to be conserving, must be based on a generating functional Φ . This functional was first considered by Luttinger and Ward [39] in the context of the thermodynamic potential, cf. [40], and later reformulated in terms of path integrals [41]. For truncated self-consistent Dyson resummations this functional method provides conserved Noether currents and the conservation of total energy and momentum at the expectation value level. In our previous paper [15] we extended the concept to the real-time Green function technique and relativistic systems, constructing conserved 4-currents and local energy-momentum tensor for any chosen approximation to the Φ functional. While Φ -derivable Dyson resummations formulated in terms of the integro-differential Kadanoff-Baym (KB) equations indeed provide *exact* conservation laws, these equations are usually not directly solvable. Therefore many applications involve further approximations to the KB equations: the *gradient* approximation and often the *quasi-particle* approximation leading to differential equations of mean field and transport type. Any improvement of the quasi-particle approximation beyond the mean-field level, e.g., through inclusion of energy-momentum-dependent self-energies, again leads to difficulties with conservation laws. Various attempts to remedy this problem were undertaken, see refs. [35, 42–47] and references therein. An essential progress within the quasi-particle approximation was achieved by the ansätze of refs. [35, 44].

Interested in the dynamics of particles with broad mass width like resonances we like to discuss the question of conservation laws for transport problems at a much more general level, than usually considered. We call this the *quantum transport* level. It completely avoids the quasi-particle approximation, and solely rests on the first-order gradient approximation of the KB equations. This concept was first addressed by Kadanoff and Baym [2] in the chapter “Slowly varying disturbances”, Eqs. (9-25). Motivated by applications for the description of heavy-ion collisions further attempts were recently suggested [18–23] based on the so called Botermans–Malfliet (BM) substitution [10]. Within the BM choice of the quantum kinetic equations a number of desired properties including an H-theorem for a local entropy current related to these equations were derived [18],

however no strict realization of the conservation laws for the Noether currents were obtained [18, 20]. Due to the approximation steps involved one may expect the quantum transport equations both, in the KB and BM forms, to possess only approximate conservation laws though in line with the level of approximation. Such approximate nature of conservation laws may be well acceptable theoretically. Nevertheless, both from a principle perspective and also from a practical point of view this situation is less satisfactory. Quantum kinetic equations which possess exact conservation laws related to the symmetries of the problem could serve as a natural extension of the quasiparticle transport phenomenology to broad resonances, e.g. applicable to high energy heavy ion collisions.

In this paper we give a proof that the quantum kinetic equations in the form originally derived by Kadanoff and Baym in fact possess the generic feature of exact conservation laws at the expectation value level. This holds provided all self-consistent self-energies are generated from a Φ -functional and all possible memory effects due to internal vertices within the self-energy diagrams are also consistently expanded to first-order gradients.

In sect. 2 we review the derivation of the quantum kinetic equations in a notation suitable for our later derivation of the conservation laws in sect. 3. Sect. 4 deals with the general gradient approximation and its representation in terms of diagrams. Finally, in sect. 5 within the Φ -derivable method we give a diagrammatic proof of the exact conservation laws of the quantum kinetic equations for the KB choice.

We restrict the presentation to physical systems described by complex quantum fields of different constituents interacting via local couplings. The kinematics can be either relativistic or non-relativistic. Extension to real boson fields, as well as to relativistic fermions is straight forward though tedious in the latter case. We also exclude theories with derivative couplings.

2. KADANOFF–BAYM EQUATIONS AND COMPLETE GRADIENT APPROXIMATION

We assume the reader to be familiar with the real-time formulation of non-equilibrium field theory on the so called closed time contour, Fig. 1. Since we will deal with general multi-point functions we use the more con-

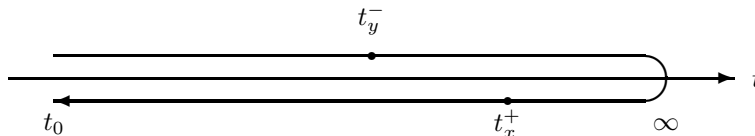


FIG. 1. Closed real-time contour with two external points x, y .

venient $\{-+\}$ contour-vertex notation of refs. [4, 18]. Some rules are summarized in Appendix A.1. The set of coupled KB equations on the time contour in $-+$ notation¹ reads

$$\begin{aligned} & (G_0^{-1}(-i\partial_1) - G_0^{-1}(-i\partial_2)) G^{-+}(1, 2) \\ & = \int_{\mathcal{C}} d3 (\Sigma(1^-, 3)G(3, 2^+) - G(1^-, 3)\Sigma(3, 2^+)) \equiv \mp C(1^-, 2^+) \end{aligned} \quad (1)$$

with Fourier transform of the inverse free Green function

$$G_0^{-1}(p) = \begin{cases} p^2 - m^2 & \text{for relativistic bosons} \\ p_0 - \mathbf{p}^2/(2m) & \text{for non-rel. fermions or bosons.} \end{cases} \quad (2)$$

Here and below the upper/lower signs refer to fermions or bosons respectively, G_0 and G correspondingly denote the free and full Green functions, labels for the different species and internal quantum numbers are suppressed. The driving term on the r.h.s. of Eq. (1), summarized by C , is a functional of the Green functions through the self-energies Σ contour folded with G . The real-time integration contour, cf. Fig. 1, is denoted by \mathcal{C} . The step towards transport equations is provided by introducing the four-dimensional Wigner transforms for all two-point functions through

$$F(x, y) = \int \frac{d^4 p}{(2\pi)^4} e^{-ip(x-y)} F\left(\frac{x+y}{2}, p\right). \quad (3)$$

The KB Eq. (1) then transforms to

$$v^\mu \partial_\mu(\mp i) G^{-+}(X, p) = C^{-+}(X, p; \{G\}) \quad \text{with} \quad v^\mu = \frac{\partial}{\partial p_\mu} G_0^{-1}(p), \quad (4)$$

where the r.h.s. is also expressed in terms of the Wigner transforms of all Green functions through (3). The final step is to expand the complicated r.h.s. of Eq. (4) to the first-order gradients. Then the *local* part of this r.h.s., $C_{(\text{loc})}^{-+}$, consists of *non-gradient terms*, where one replaces the different mean positions $(x_i + x_j)/2$ occurring in the various Green functions by the externally given mean position X of the l.h.s., i.e. $X = (x_1 + x_2)/2$ and evaluates the diagrams as in momentum representation. The corrections

¹The numbers 1, 2 and 3 provide short hand notation for space-time coordinates x_1, x_2 and x_3 , respectively, including internal quantum numbers. With superscript, like 1^- and 2^+ , assigned to them, they denote contour coordinates with $-$ and $+$ specifying the placement on the time or anti-time ordered branch. Decomposed to the two branches the contour functions are denoted as $F^{kl}(1, 2) = F(1^k, 2^l)$ with $k, l \in \{-, +\}$. The match to the notation used, e.g., in refs. [2, 7] is given by $F^{-+} = F^<$; $F^{+-} = F^>$; $F^{--} = F^c$; $F^{++} = F^a$.

for the displacement to the true coordinates of each Green function are then accounted for to the first order in the gradients. Here we simply abbreviate the gradient terms by a \diamond operator acting on the *local* diagram expression

$$v^\mu \partial_\mu (\mp i) G^{-+}(X, p) = (1 + \frac{i}{2} \diamond) \{ C_{(\text{loc})}^{-+}(X, p) \}, \quad (5)$$

where

$$C_{(\text{loc})}^{-+}(X, p) = C^{-+}(X, p; \{G_{(\text{loc})}\}), \quad (6)$$

is a functional of the local Green functions $G_{(\text{loc})} \equiv G(X, p)$. Here and for all further considerations below, both, Green functions $G(X, p)$ and self-energies $\Sigma(X, p)$, whenever quoted in their Wigner function form, are taken in *local* approximation, i.e. with X given by the external coordinate and $\Sigma(X, p)$ void of any gradient correction terms. The explicit definition of the \diamond -operator is deferred to sect. 4. All what we need to know at this level is that it consists of terms where in the diagrams defining $C_{(\text{loc})}$ pairs of Green functions are replaced by their space-time and momentum derivatives, respectively, just leading to equations linear in space-time gradients. Naturally the result of the \diamond -operation depends on the explicit form, i.e. diagrammatic structure, of the functional on which it operates. Therefore for the non-gradient term in Eq. (5), which defines the *local* collision term

$$C_{(\text{loc})}^{-+} \underset{\text{diagram}}{=} \mp \Sigma^{-k}(X, p) \sigma_{kl} G^{l+}(X, p) - (\mp) G^{-k}(X, p) \sigma_{kl} \Sigma^{l+}(X, p) \quad (7)$$

$$\underset{\text{value}}{=} \underbrace{\mp i \Sigma^{-+}(X, p) i G^{+-}(X, p)}_{\text{gain}} - \underbrace{(\mp) i G^{-+}(X, p) i \Sigma^{+-}(X, p)}_{\text{loss}}, \quad (8)$$

we give both, the diagram expression (7) and the normally quoted *value* expression (8). The latter simplifies due to a cancellation of terms which however survive for the order sensitive gradient operation. Here $\sigma_{ik} = \sigma^{ik} = \text{diag}(1, -1)$ defines the “contour metric”, which accounts for the integration sense, and summation over the contour labels $k, l \in \{-, +\}$ is implied, cf. (A.2) ff.

The above quantum kinetic equation (5) has to be supplemented by a *local* Dyson equation for the retarded Green function [2]

$$(G^R(X, p))^{-1} = (G_0^R(p))^{-1} - \Sigma^R(X, p), \quad (9)$$

which together with Eq. (5) provides the simultaneous solution to G^{+-} . The full retarded Green function G^R depends on the retarded self-energy $\Sigma^R = \Sigma^{--} - \Sigma^{-+} = \Sigma^{+-} - \Sigma^{++}$ again in *local* approximation. G_0^R is

the free retarded Green function. Please note that equation (9) is just algebraic although it is obtained in the framework of the first-order gradient approximation.

In most presentations of the gradient approximation to the KB equations, Eq. (5) is rewritten such that the gradient terms are subdivided into two parts, consisting of Poisson bracket terms describing drag- and back-flow effects, on the one side, and a memory collision term C^{mem} , on the other side, in cases when the self-energy contains internal vertices

$$v^\mu \partial_\mu (\mp) i G^{-+}(X, p) = \{ \text{Re} \Sigma^R, \mp i G^{-+} \} + \{ \mp i \Sigma^{-+}, \text{Re} G^R \} + C_{(\text{mem})}^{-+}(X, p) + C_{(\text{loc})}^{-+}(X, p), \quad (10)$$

where

$$\begin{aligned} \mp C_{(\text{mem})}^{-+}(X, p) &= \Sigma_{(\text{mem})}^{-k}(X, p) \sigma_{kl} G^{l+}(X, p) - G^{-k}(X, p) \sigma_{kl} \Sigma_{(\text{mem})}^{l+}(X, p) \quad (11) \\ &= -\Sigma_{(\text{mem})}^{-+}(X, p) G^{+-}(X, p) + G^{-+}(X, p) \Sigma_{(\text{mem})}^{+-}(X, p) \quad (12) \end{aligned}$$

value

and

$$\Sigma_{(\text{mem})}(X, p) = \frac{i}{2} \diamond \{ \Sigma(X, p) \}. \quad (13)$$

One may further introduce the spectral function $A(X, p) = -2\text{Im}G^R(X, p)$ determined by the retarded equation (9), as well as the four-phase-space distribution function $f(X, p)$, by means of $\mp i G^{-+}(X, p) = f(X, p)A(X, p)$, whose evolution is governed by transport Eq. (10) or equivalently by (5). This defines a generalized quantum transport scheme which is void of the usual quasi-particle assumption. The time evolution is completely determined by initial instantaneous values of the Green functions and their gradients at each space-time point, which means it is *Markovian*, since the memory part of the collision term is kept only up to first-order gradient terms. Within its validity range this transport scheme is capable to describe slow space-time evolutions of particles with broad damping width, such as resonances, within a transport dynamics, now necessarily formulated in the four-dimensional phase-space.

Depending on the questions raised, the above separation (10) may not be always useful. For the derivation of the conservation laws only a unified treatment of both, the Poisson brackets and memory collision terms, reveals the symmetry among these terms, which then displays the necessary cancellation of certain contributions such that the conservation laws emerge. Therefore, in the forthcoming considerations we will mostly refer to the quantum kinetic equation in the form (5).

3. CONSERVATION LAWS

Conservations of charge and energy–momentum result from taking the charge or four–momentum weighted traces of the transport equations (5). These traces include the integration over four–momentum, as well as sums over internal quantum numbers and all types of species a with charges e_a

$$\begin{aligned} \partial_\mu \sum_a \int \frac{d^4 p}{(2\pi)^4} \left(\frac{e_a}{p^\nu} \right) v^\mu (\mp i) G_a^{-+}(X, p) \\ = \sum_a \int \frac{d^4 p}{(2\pi)^4} \left(\frac{e_a}{p^\nu} \right) \left(1 + \frac{i}{2} \diamond \right) \left\{ C_{a(\text{loc})}^{--}(X, p) \right\} \equiv \begin{pmatrix} Q(X) \\ T^\nu(X) \end{pmatrix}. \end{aligned} \quad (14)$$

The the charge and four–momentum leaks on the r.h.s, abbreviated as Q and T^ν , can be represented by closed diagrams, where the two end points (x_1^- and x_2^+ in Eq. (1)) coalesce, i.e. $x_1 = x_2 = X$. In coordinate representation the r.h.s. corresponds to contour integrals of the type (A.7) - (A.9) for which entirely retarded terms drop out. Therefore, one even can place the two end points on the same contour side (respecting the fixed order for Tad-pole terms). For definiteness we have chosen the time ordered ($-$) branch. The external point $x_1^- = x_2^- = X$ is then the reference point with respect to which the gradients are to be evaluated. In line with causality requirements this reference point $X = (t, \mathbf{x})$ is also the *retarded point*. This implies that in a real-time contour representation any contribution to (14) from internal integrations with physical times larger than t drops out, cf. [32, 8]. Using the explicit form of the contour metric σ (cf. Eqs. (A.3) and (A.4)) one obtains

$$C_{a(\text{loc})}^{--}(X, p) = \mp (\Sigma_{-k}^a(X, p) G_a^{k-}(X, p) - G_a^{-k}(X, p) \Sigma_{k-}^a(X, p)). \quad (15)$$

In the proof given in sect. 5 we show that the local parts of the r.h.s. of (14) as given by

$$\begin{pmatrix} Q_{\text{loc}}(X) \\ T_{\text{loc}}^\nu(X) \end{pmatrix} = \sum_a \int \frac{d^4 p}{(2\pi)^4} \left(\frac{e_a}{p^\nu} \right) C_{a(\text{loc})}^{--}(X, p) \quad (16)$$

entirely drop out. Also the gradient terms of Q cancel, while the gradients of the T^ν term compile to a complete divergence

$$Q(X) \equiv 0, \quad T^\nu(X) = g^{\mu\nu} \partial_\mu (\mathcal{E}^{\text{pot}}(X) - \mathcal{E}^{\text{int}}(X)), \quad (17)$$

provided the self-energies are derived from a so called Φ -functional [38]. This implies exact conservation laws for the Noether currents and the energy–momentum tensor given by

$$\partial_\mu J^\mu(X) = 0, \quad \partial_\mu \Theta_{\text{loc}}^{\mu\nu}(X) = 0 \quad \text{with} \quad (18)$$

$$J^\mu(X) = \sum_a \int \frac{d^4p}{(2\pi)^4} e_a v^\mu(\mp i) G_a^{-+}(X, p), \quad (19)$$

$$\Theta_{\text{loc}}^{\mu\nu}(X) = \sum_a \int \frac{d^4p}{(2\pi)^4} v^\mu p^\nu(\mp i) G_a^{-+}(X, p) + g^{\mu\nu} (\mathcal{E}_{\text{loc}}^{\text{int}}(X) - \mathcal{E}_{\text{loc}}^{\text{pot}}(X)). \quad (20)$$

Here G is the self-consistent propagator solving the coupled set of quantum transport equations (5) and (9). Furthermore, $\Theta_{\text{loc}}^{\mu\nu}(X)$ is the *local* version of energy-momentum tensor which for the Φ -derivable approximation to the KB equations has been constructed in our previous papers [15, 18]. Thereby, $\mathcal{E}_{\text{loc}}^{\text{int}}(X)$ and $\mathcal{E}_{\text{loc}}^{\text{pot}}(X)$ define the interaction and single-particle potential energy densities, respectively, also taken in the local approximation.

In the subsequent sections we formally define the complete first-order gradient expansion for any two point function, which contains internal vertices, and specify the corresponding diagrammatic rules. Finally, in sect. 5 we prove the conservation laws (18), using the Φ -derivable properties and the gradient rules.

4. COMPLETE GRADIENT APPROXIMATION

Let $M(1, 2)$ be any two-point function with complicated internal structure. We are looking for its Wigner function $M(X, p)$ with $X = \frac{1}{2}(x_1 + x_2)$ to first-order gradient approximation. The zero-order term is just given by evaluating $M(1, 2)$ with the Wigner functions of *all* Green functions taken at the same space-time point $X = (x_1 + x_2)/2$ and the momentum integrations being done as in the momentum representation of a homogeneous system. To access the gradient terms related to any Green function $G(i, j)$ involved in $M(1, 2)$, its Wigner function $G(\frac{1}{2}(x_i + x_j), p)$ is to be Taylor expanded with respect to the reference point $X = (x_1 + x_2)/2$, i.e.

$$G\left(\frac{x_i + x_j}{2}, p\right) \approx G(X, p) + \frac{1}{2} [(x_i^\mu - x_1^\mu) + (x_j^\mu - x_2^\mu)] \frac{\partial}{\partial X^\mu} G(X, p). \quad (21)$$

Both the space derivatives of Green functions and the factors $(x_i - x_1)$ and $(x_j - x_2)$ accompanying them can be taken as special two-point functions, and we therefore assign them special diagrams

$$\overline{\overline{i \quad j}} = \frac{1}{2} (\partial_i + \partial_j) G(i, j) \longrightarrow \partial_X G(X, p), \quad (22)$$

$$- \overline{\overline{i \quad j}} = -i (x_i - x_j) \longrightarrow -(2\pi)^4 \frac{\partial}{\partial p} \delta(p) \quad (23)$$

with the corresponding Wigner functions at the right hand side. Then the gradient terms of a complicated two-point function (given in different notation) can graphically be represented by the following two diagrams on the r.h.s.

$$\diamond \{M(1, 2)\} = \diamond \begin{array}{c} \square \\ \text{---} M \text{---} \\ \bullet \quad \bullet \\ 1 \quad 2 \end{array} \equiv \diamond \begin{array}{c} \diamond M \\ \bullet \quad \bullet \\ 1 \quad 2 \end{array} = \begin{array}{c} \overset{3}{\curvearrowright} \quad \overset{4}{\curvearrowleft} \\ \text{---} M' \text{---} \\ \bullet \quad \bullet \\ 1 \quad 2 \end{array} + \begin{array}{c} \overset{3}{\curvearrowleft} \quad \overset{4}{\curvearrowright} \\ \text{---} M' \text{---} \\ \bullet \quad \bullet \\ 1 \quad 2 \end{array} \quad (24)$$

Here the diamond operator \diamond , as above, formally defines the gradient approximation of the two-point function M to its right with respect to the two external points $(1, 2)$ displayed by full dots. The diagrammatic rules are then the following. For any $G(3, 4)$ in M , take the spatial derivative $\partial_X G(X, p)$ (double line) and construct the two diagrams, where external point 1 is linked to 3 by an oriented dashed line, and where point 2 is linked to 4, respectively. Interchange of these links provides the same result. Here M' is a four-point function generated by opening $M(1, 2)$ with respect to any propagator $G(3, 4)$, i.e.

$$M'(1, 2; 3, 4) = \mp \frac{\delta M(1, 2)}{\delta iG(4, 3)}. \quad (25)$$

The diagrams in Eq. (24) are then to be evaluated in the local approximation, i.e. with all Wigner Green functions taken at the same space-time point X . The dashed line (23) adds a new loop integration to the diagram, which, if integrated, leads to momentum derivatives of the Green functions involved in that loop. Both, double and dashed lines have four-vector properties, and the rule implies a four-scalar product between them.

The explicit properties of the dashed line (23) permit to decompose it into two or several dashed lines through the algebra

$$\begin{array}{c} \text{---} \leftarrow \text{---} \\ 1 \quad 3 \end{array} = \begin{array}{c} \text{---} \leftarrow \text{---} \\ 1 \quad 2 \end{array} + \begin{array}{c} \text{---} \leftarrow \text{---} \\ 2 \quad 3 \end{array} \quad \text{and} \quad \begin{array}{c} \bullet \\ \text{---} \circ \text{---} \\ \bullet \end{array} = 0. \quad (26)$$

In momentum-space representation these rules correspond to the partial integration. They imply that $\diamond \{M(1, 2)\} = 0$, if M contains no internal vertices. Applying rule (26) to the convolution of two two-point functions

$$C(1, 2) = \int_c d3A(1, 3)B(3, 2) \quad (27)$$

leads to the following convolution theorem for the gradient approximation

$$\begin{aligned}
\Diamond\{C(X, p)\} &= \Diamond \left\{ \begin{array}{c} \text{---} \blacktriangleleft \text{A} \blacktriangleright \text{---} \blacktriangleleft \text{B} \blacktriangleright \text{---} \\ \text{---} \end{array} \right\} \\
&= \begin{array}{c} \text{---} \blacktriangleleft \text{A} \blacktriangleright \text{---} \text{---} \partial_X \text{B} \blacktriangleright \text{---} \\ \text{---} \end{array} + \begin{array}{c} \text{---} \partial_X \text{A} \blacktriangleright \text{---} \blacktriangleleft \text{B} \blacktriangleright \text{---} \\ \text{---} \end{array} \\
&\quad + \begin{array}{c} \text{---} \blacktriangleleft \text{A} \blacktriangleright \text{---} \blacktriangleleft \text{B} \blacktriangleright \text{---} \\ \text{---} \end{array} + \begin{array}{c} \text{---} \blacktriangleleft \text{A} \blacktriangleright \text{---} \blacktriangleleft \text{B} \blacktriangleright \text{---} \\ \text{---} \end{array} \quad (28)
\end{aligned}$$

$$\begin{aligned}
&= \{A(X, p), B(X, p)\} \\
&\quad + A(X, p) \Diamond\{B(X, p)\} + \Diamond\{A(X, p)\} B(X, P). \quad (29)
\end{aligned}$$

Besides the standard Poisson bracket expression $\{A, B\}$ it leads to further gradients within each of the two functions (note that the \Diamond operator acts only on the two-point function in the immediate braces to its right). Applied to the r.h.s. of Eq. (5), this rule indeed provides the decomposition into Poisson bracket and memory terms for the more conventional formulation of the quantum kinetic equation (10).

5. Φ -DERIVABLE SCHEME AND EXACT CONSERVATION LAWS

In this section we first review the Φ -derivable properties at the level of self-consistent Dyson or KB equations, then proceed towards the implications for the quantum kinetic equations (5) and to the proof of the corresponding exact conservation laws (18).

In a Φ -derivable scheme the self-energies are generated from a functional $\Phi\{G, \lambda\}$ through the following functional variation², cf. [15]

$$-i\Sigma(x, y) = \mp \frac{\delta i\Phi\{G, \lambda\}}{\delta iG(y, x)} \times \begin{cases} 2 & \text{for real fields} \\ 1 & \text{for complex fields} \end{cases}. \quad (30)$$

The Φ functional itself is given by two-particle irreducible ($2PI$) closed diagrams in terms of *full* Green functions of the underlying field theory, i.e.

$$i\Phi\{G, \lambda\} = \left\langle \exp \left(i \int_{\mathcal{C}} d^4x \lambda(x) \mathcal{L}^{\text{int}} \right) \right\rangle_{2PI}. \quad (31)$$

²Here we include also the rule for real fields, upper/lower signs refer to fermions/bosons

The interaction strength $\lambda(x)$, the physical value of which is $\lambda = 1$, allows the definition of the interaction energy density

$$\mathcal{E}^{\text{int}}(x) = \left\langle -\widehat{\mathcal{L}}^{\text{int}}(x) \right\rangle = - \left. \frac{\delta i\Phi}{\delta i\lambda(x)} \right|_{\lambda=1}. \quad (32)$$

The single-particle potential energy density is defined as

$$\mathcal{E}^{\text{pot}}(x) = \frac{1}{2} \int_{\mathcal{C}} d^4y [\Sigma(x, y)(\mp i)G(y, x) + (\mp i)G(x, y)\Sigma(y, x)] \quad (33)$$

for complex fields. The local approximants to both \mathcal{E}^{int} and \mathcal{E}^{pot} enter the energy-momentum tensor (18).

The diagrammatic series of Φ given by Eq. (31) can be truncated at any level. Keeping the variational property (30), this defines a truncated self-consistent scheme for the KB equations (1). The so constructed self-energies lead to a coupling between the different species a , which obey detailed balance³. It has been shown [38], see also [15], that such a self-consistent scheme is exactly conserving at the expectation value level and thermodynamically consistent at the same time.

A prominent example is the particle-hole ring resummation in Fermi liquid theory in the limit of zero range four-fermion coupling with the following diagrams

$$\Phi = \frac{1}{2} \text{diagram}_1 + \frac{1}{4} \text{diagram}_2 + \sum_{n>2} \frac{1}{2n} \text{diagram}_3, \quad (34)$$

$$\mathcal{E}^{\text{int}}(X) = \frac{1}{2} \text{diagram}_1 + \frac{1}{2} \text{diagram}_2 + \sum_{n>2} \frac{1}{2} \text{diagram}_3, \quad (35)$$

$$\Sigma(x, y) = \text{diagram}_1 + \text{diagram}_2 + \sum_{n>2} \text{diagram}_3 \quad (36)$$

Here n counts the number of vertices in the diagram, the full dots denote the external points X and (x, y) . Note that compared to $\mathcal{E}^{\text{int}}(X)$ all coordinates are integrated in Φ , and therefore its diagrams attain an extra combinatorial factor $1/n$ [39]. These diagrams illustrate various levels of approximation. Restricting Φ just to the one-point term provides

³generalizing the special recipes for broad resonances given in ref. [48]

the Hartree approximation. From the two-point level on the collision term becomes finite, which also leads to finite damping widths of the particles. Terms, where Φ has more than two internal vertices, give rise to memory contributions to the self-energies, cf. (10), due to the intermediate times of the internal vertices in $\Sigma(x, y)$. For this example the memory terms give rise to the famous $T^3 \ln T$ term in the specific heat of liquid ${}^3\text{He}$ [49–51] at low temperatures T .

It is possible to transcribe the variational rules to the local approximation defining a local Φ -functional replacing everywhere G by its local approximant, cf. (6),

$$\Phi_{\text{loc}}(X) = \Phi\{G, \lambda^\mp\} \Big|_{G=G_{\text{loc}}=G(X,p)}. \quad (37)$$

Here X is an externally given parameter defining the reference point for the local approximation, and λ^\mp denotes the scaling factors of the vertices on the time or anti-time ordered branches of the contour. The variational rules (30) and (32) then transcribe to

$$-i\Sigma_{ik}(X, p) = \mp \frac{\delta i\Phi_{\text{loc}}(X)}{\delta iG^{ki}(X, p)} \times \begin{cases} 2 & \text{for real fields} \\ 1 & \text{for complex fields} \end{cases}, \quad (38)$$

$$\mathcal{E}_{\text{loc}}^{\text{int}}(X) = - \frac{\delta i\Phi_{\text{loc}}(X)}{\delta i\lambda^-} \Big|_{\lambda^-=1} = \frac{\delta i\Phi_{\text{loc}}(X)}{\delta i\lambda^+} \Big|_{\lambda^+=1}. \quad (39)$$

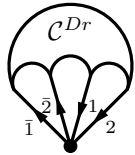
In order to prove that the exact conserving properties indeed survive in the first-order gradient expansion (5), we shall use the conserving properties of the Φ diagrams at each internal vertex together with the variational property (30).

5.1. Properties of diagrams

We return to the r.h.s. terms of the conservation laws (16). Due to the variational property (30), it is evident that they are given by closed diagrams of the same topology as those of Φ , however, with one point not contour integrated but placed on the time-ordered ($-$) branch with coordinate X . To further reveal this relation between the “two-point” representation, as given by the r.h.s. of Eq. (16), and the *retarded* one-point representation of Φ with respect to a chosen reference point X^- , we have to resolve the internal structure of the different diagrams contributing to Φ . Therefore, we first decompose Φ into the terms of different diagrammatic topology

$$i\Phi_{\text{loc}}(X) = \sum_D i\Phi_{\text{loc}}^D(X) \quad (40)$$

and discuss the features of any such term Φ_{loc}^D . We then enumerate the different vertices ($r = 1, \dots, n_\lambda$) in each Φ_{loc}^D , n_λ denoting the number of vertices in Φ_{loc}^D . For each such retarded vertex r^- we define a one-point function $\Phi_{\text{loc}}^D(X; r^-)$, which is obtained by integration and $\{-+\}$ summation over all other vertices except r and by putting r on the time ordered ($-$) branch at coordinate X . Subsequently we enumerate the few Green functions attached to r^- and label them as G_γ^{-k} or $G_{\bar{\gamma}}^{k-}$, depending on the line sense pointing towards or away from r^- , respectively. Thus, the retarded function $\Phi^D(X; r^-)$ can be represented by a diagram, where the retarded point is explicitly pulled out. We draw this as a kind of “parachute” diagram which in *local* approximation becomes

$$\begin{aligned}
 i\Phi_{\text{loc}}^D(X; r^-) &= \text{Diagram} \\
 &= \int \frac{d^4 p_1}{(2\pi)^4} \cdots \frac{d^4 \bar{p}_1}{(2\pi)^4} \cdots \mathcal{C}_{k_1 \dots \bar{k}_1}^{Dr}(X; p_1, \dots, \bar{p}_1, \dots) \\
 &\quad \times (\mp i) G_1^{-k_1}(X, p_1) \cdots i G_{\bar{1}}^{k_1-}(X, \bar{p}_1) \cdots \quad (41)
 \end{aligned}$$


The diagram shows a central point labeled r^- . Above it is a semi-circular canopy labeled \mathcal{C}^{Dr} . From r^- , four lines (suspension cords) extend upwards and outwards, each ending in an arrow pointing towards r^- . The lines are labeled with indices $\bar{1}$, 1 , 2 , and $\bar{2}$ from left to right.

The Green functions attached to the external retarded point r^- , form the “suspension cords”. The “canopy” part \mathcal{C}^{Dr} specifies the rest of the diagram which is not explicitly drawn⁴. Here all Green functions are taken in the local approximation, i.e. with coordinate X given by the reference point. From the variational principle (30) it is clear that $\Phi^D(X; r^-)$ can be interpreted in different equivalent ways depending on which line attached to r^- being opened

$$i\Phi_{\text{loc}}^D(X; r^-) = \mp \int \frac{d^4 p}{(2\pi)^4} G_\gamma^{-k}(X, p) \Sigma_{k-}^{Dr\gamma}(X, p) \quad (42)$$

$$= \mp \int \frac{d^4 p}{(2\pi)^4} \Sigma_{-k}^{Dr\bar{\gamma}}(X, p) G_{\bar{\gamma}}^{k-}(X, p), \quad (43)$$

Here G_γ (or $G_{\bar{\gamma}}$) is one of the suspension cords with the arrow pointing towards (or away) from r . *No* summation over γ is implied by these relations! The self-energy terms $\Sigma^{Dr\gamma}$ and $\Sigma^{Dr\bar{\gamma}}$ are given by those subdiagrams of

⁴For definiteness we have drawn a diagram with 4 propagators linking to the retarded point r^- . All considerations, however, are independent of the coupling scheme which can even vary from vertex to vertex. For simple Φ diagrams, such as those with only two vertices at all, the canopy part reduces simply to a single point, cf. the second diagram in Eq. (34).

$\Phi_{\text{loc}}^D(r^-)$ complementary to G_γ and $G_{\bar{\gamma}}$, respectively. According to the variational rule (30) they contribute to the self-energy of a given species a as

$$-i\Sigma_{k-}^a(X, p) = \mp \frac{\delta i\Phi_{\text{loc}}}{\delta iG_a^{-k}(X, p)} = - \sum_D \sum_{r \in D} \sum_\gamma i\Sigma_{k-}^{Dr\gamma}(X, p) \delta_{a\gamma} \quad (44)$$

and similarly for $\Sigma_{-k}^{Dr\bar{\gamma}}$ leading to Σ_{-k}^a . The Kronecker symbol $\delta_{a\gamma}$ projects on species a . The summation in r runs over all vertices in the Φ_{loc}^D diagram. It is clear that each Green function in Φ_{loc}^D appears once in the count of Σ_{k-} and once in the count of Σ_{-k} . This precisely matches with the two terms required in Eq. (15). We further note that the variation (32) of Φ with respect to the coupling strength $\lambda(X)$ can be represented as

$$\mathcal{E}^{\text{int}}(X) = - \frac{\delta i\Phi_{\text{loc}}(X)}{\delta i\lambda^-} = - \sum_D \sum_{r \in D} \Phi_{\text{loc}}^D(X; r^-). \quad (45)$$

5.2. Charge-current conservation

The discussion above shows that any term of the local part of the charge leak $Q_{\text{loc}}(X)$ in Eq. (16) is given by a closed diagram of the same topology as the $\Phi_{\text{loc}}^D(r^-)$. Indeed, weighting $\Phi_{\text{loc}}^D(X; r^-)$ with the charges of the in- and out-going Green functions reproduces piece by piece the local gain and loss terms in Eq. (15). The sum over all possible retarded vertices r in diagram D and the sum over all diagrams indeed exactly construct Q_{loc} as

$$\begin{aligned} Q_{\text{loc}}(X) &= \int \frac{d^4p}{(2\pi)^4} \sum_a e_a C_{a, \text{loc}}^{--}(X, p) \\ &= \sum_D \sum_{r \in D} \left(\underbrace{\sum_{\bar{\gamma}} e_{\bar{\gamma}} - \sum_{\gamma} e_{\gamma}}_{\equiv 0} \right) i\Phi_{\text{loc}}^D(X; r^-). \end{aligned} \quad (46)$$

Since the charge sum vanishes at each vertex, Q_{loc} identically vanishes.

The fact that the local collision term part vanishes is indeed trivial. The point here is that the cancellation occurs diagram by diagram in terms of $\Phi_{\text{loc}}^D(X; r^-)$. This has the important consequence that the gradient terms exactly cancel out, too, i.e.

$$\sum_a \int \frac{d^4p}{(2\pi)^4} e_a \diamond C_{a, \text{loc}}^{--}(X, p) = \diamond Q_{\text{loc}} \equiv 0, \quad (47)$$

since they are generated by applying linear differential operations to the integrand of $\Phi_{\text{loc}}^D(X; r^-)$, while the charge factors are constants. There-

fore, we have verified that $Q(X) \equiv 0$. This proves current conservation, where the current has the original Noether form. This proof applies to any conserved current of the underlying field theory, which relates to a global symmetry.

5.3. Energy-Momentum Tensor

In a similar way as above the four-momentum weighted terms become

$$T_{\text{loc}}^\nu(X) = \sum_D \sum_{r \in D} \int \frac{d^4 p_1}{(2\pi)^4} \cdots \frac{d^4 \bar{p}_1}{(2\pi)^4} \cdots \left(\underbrace{\sum_{\bar{\gamma}} p_{\bar{\gamma}}^\nu - \sum_{\gamma} p_{\gamma}^\nu}_{\equiv 0} \right) \quad (48)$$

$$\times \mathcal{C}_{k_1 \dots \bar{k}_1}^{Dr} (X; p_1, \dots, \bar{p}_1, \dots) (\mp i) G_1^{-k_1}(X, p_1) \cdots i G_1^{\bar{k}_1}(X, \bar{p}_1) \cdots$$

Here we have used the integrand form (41) of the parachute diagram $\Phi(X; r^-)$, since now the weights are momentum dependent. This local collision-term part again drops out in the same way as above. However, the gradient correction to T^ν now involves momentum derivatives which can act on the p^ν -factors in Eq. (14) through partial integrations. Indeed, *only* those momentum derivatives survive that act on any of the p^ν -factors, since momentum derivatives acting on any of the Green functions leave the vanishing pre-factor in Eq. (48) untouched.

The actual evaluation of the gradients is subtle and depends on the detailed topological structure of the diagram. For this purpose we use the diagrammatic rules (24) for the gradient terms with the double line as $\partial^\mu G(X, p)$, dashed lines as $\propto \partial \delta(p) / \partial p^\mu$. For the subsequent analysis we also introduce a new diagrammatic element, a genuine two-point function which gives the four-momentum p^ν -factor “flowing” through the line

$$p^\nu = \text{wavy line with } \nu \text{ label} \quad \text{with} \quad \text{dashed circle with } \mu \text{ label} = - \text{dashed circle with } \mu \text{ label} = \frac{\partial p^\nu}{\partial p_\mu} = g^{\mu\nu}. \quad (49)$$

The last relation results from partial integration and depends only on the sense of the dashed line.

Note that the p^ν factors in the r.h.s. of Eq. (14) occur outside the gradient expression. Using the convolution theorem (28), we first pull the p^ν factors into the gradient terms in the following manner (using $g^{\mu\nu} = \partial p^\nu / \partial p_\mu$)

$$\diamond \{ \Sigma \cdot G \} p^\nu - p^\nu \diamond \{ G \cdot \Sigma \} \\ = \underbrace{g^{\mu\nu} \partial_\mu (\Sigma \cdot G + G \cdot \Sigma)}_{\mp E_1^\nu(X, p)} + \underbrace{\{ \Sigma \cdot G \cdot p^\nu - p^\nu \cdot G \cdot \Sigma \}}_{\mp E_2^\nu(X, p)}. \quad (50)$$

Please, note the order of the terms under the \diamond operator as they do *not commute!* The first term, E_1^ν , arose from the Poisson bracket term in Eq. (28). In accord with Eq. (33), the four-momentum integration obviously provides the potential energy density term

$$\frac{i}{2} \int \frac{d^4 p}{(2\pi)^4} E_1^\nu(X, p) = g^{\mu\nu} \partial_\mu \mathcal{E}_{\text{loc}}^{\text{pot}}(X) \quad (51)$$

of the energy–momentum tensor (18).

Thus, we expect the second E_2^ν term to generate the remaining interaction energy density part $g^{\mu\nu} \mathcal{E}_{\text{loc}}^{\text{int}}(X)$ of $\Theta^{\mu\nu}$. The four-momentum integration of the E_2^ν term again leads to a coalescence of the two external points. Thus the corresponding diagrams are of the parachute type

$$\int \frac{d^4 p}{(2\pi)^4} E_2^\nu(X, p) = \sum_{D, r \in D} \left(\diamond \begin{array}{c} \text{C}^{Dr} \\ \nu \\ r^- \end{array} + \dots + \diamond \begin{array}{c} \text{C}^{Dr} \\ \nu \\ r^- \end{array} \right), \quad (52)$$

where both reference points for the gradient expansion coalesce to r^- , cf. Eqs. (42) and (43). Here the p^ν factor occurs in sequence at each of the suspension cords reflecting the sum over γ and $\bar{\gamma}$. In order to exploit the fact that thereby $\sum_\gamma p_\gamma^\nu - \sum_{\bar{\gamma}} p_{\bar{\gamma}}^\nu$ vanishes, all the different diagrams in the bracket in (52) have to be evaluated in the same way. Omitting all labels, one obtains for the first diagram in Eq. (52)

$$\begin{aligned} \diamond \begin{array}{c} \text{C} \\ \nu \\ r^- \end{array} &= \begin{array}{c} \text{C}' \\ \nu \\ r^- \end{array} + \begin{array}{c} \text{C}' \\ \nu \\ r^- \end{array} \\ &+ \begin{array}{c} \text{C} \\ \nu \\ r^- \end{array} + \begin{array}{c} \text{C} \\ \nu \\ r^- \end{array} + \dots + \begin{array}{c} \text{C} \\ \nu \\ r^- \end{array} \quad (53) \end{aligned}$$

$$\begin{aligned} \Rightarrow & 2 \begin{array}{c} \partial_x \text{C} \\ \nu \\ r^- \end{array} + 2 \begin{array}{c} \text{C} \\ \nu \\ r^- \end{array} \quad (54) \end{aligned}$$

where $\mathcal{C}' = \mp \delta \mathcal{C} / \delta i G$ and the four-scalar product between the double and dashed lines is implied in each diagram. The sequence (a) to (f) defines all diagrams resulting from the gradient expansion. The two diagrams (α) and (β) shown in (54) are the only ones that finally survive the p^ν sum, i.e. the sum over “suspension cords” in Eq. (52). In detail: diagrams (a) and (b) specify the gradient terms arising from the space-time derivatives acting on Green functions within the canopy part. Using addition theorem (26) the dashed lines can be first linked from the bottom point to one definitely chosen upper suspension points \mathbf{f} , as shown in diagram (α), and from there then further linked to the end points of the double line. However, the latter terms lead to p -derivatives entirely within the canopy, which finally drop out due to the vanishing p^ν sum. Diagrams (c) to (f) sequentially take the space-time gradients of the Green functions in the suspension cords converting them to a double line in each case. Also here only terms survive, where the momentum derivative acts on the p^ν factor, leading to diagram (β).

One can now compile the terms in Eq. (52) provided point \mathbf{f} is kept fixed. Then from (α) only a single term survives, namely that where the p^ν factor is on the line linking to \mathbf{f} , while from (β) each term survives. The net result leads to a common $g^{\mu\nu}$ -factor, cf. (49), times a total derivative of the entire parachute diagram, i.e.

$$\begin{aligned}
\frac{i}{2} \int \frac{d^4 p}{(2\pi)^4} E_2^\nu(X, p) &= -i \sum_{D, r \in D} g^{\mu\nu} \partial_\mu \text{ (parachute diagram) } \\
&= -i g^{\mu\nu} \partial_\mu \underbrace{\sum_{D, r \in D} i \Phi_{\text{loc}}^D(X, r^-)}_{i \frac{\delta i \Phi_{\text{loc}}^D}{\delta i \lambda^-}} \quad (55) \\
&= -g^{\mu\nu} \partial_\mu \mathcal{E}^{\text{int}}(X) \quad (56)
\end{aligned}$$

from Eq. (45). Together with relation (51), this gives

$$T^\nu(X) = -\partial^\nu (\mathcal{E}_{\text{loc}}^{\text{int}}(X) - \mathcal{E}_{\text{loc}}^{\text{pot}}(X)) \quad (57)$$

for the r.h.s of conservation law (14). It is seen to be determined by the full divergence of the difference between the interaction energy and single-particle potential energy densities defined by Eqs. (32) and (33), now however evaluated in the *local* approximation, i.e. with no gradient

terms in the Wigner representation:

$$\begin{aligned} \mathcal{E}_{\text{loc}}^{\text{pot}}(X) &= \int \frac{d^4p}{(2\pi)^4} [\text{Re}\Sigma^R(X, p)(\mp i)G^{-+}(X, p) \\ &\quad + \text{Re}G^R(X, p)(\mp i)\Sigma^{-+}(X, p)] \end{aligned} \quad (58)$$

$$\begin{aligned} &= - \int \frac{d^4p}{(2\pi)^4} \left[\text{Re} \left(\frac{\delta\Phi_{\text{loc}}}{\delta iG(X, p)} \right)^R iG^{-+}(X, p) \right. \\ &\quad \left. + \text{Re}G^R(X, p) \left(\frac{\delta\Phi_{\text{loc}}}{\delta iG(X, p)} \right)^{-+} \right]. \end{aligned} \quad (59)$$

Here the superscript R denotes the corresponding retarded function. For each diagram Φ_{loc}^D the contribution to $\mathcal{E}_{\text{loc}}^{\text{int}}(X)$ results from the corresponding terms of $\mathcal{E}_{\text{loc}}^{\text{pot}}(X)$ just by scaling each term by the number of vertices n_λ over the number of Green functions n_G .

6. CONCLUDING REMARKS

The quantum transport equations in the form originally proposed by Kadanoff and Baym, (5) or equivalently (10), have very pleasant generic features. As possible memory effects in the collision term are to be included only up to first-order space-time gradients, they are local in time to the extent that only the knowledge of the Green functions and their space-time and four-momentum derivatives at this time is required to determine the future evolution. They further preserve the retarded relations among the various real-time components of the Green function.

In this paper we have shown that they also possess *exact* rather than approximate conservation laws, related to global symmetries of the system, if the scheme is Φ -derivable. The same Noether currents and the same energy-momentum-tensor [15] as those for the original KB equations, however now in their local approximation forms, are exactly conserved for the complete gradient-expanded KB equation, i.e. the quantum transport equations (5). Thus,

$$\partial_\mu J^\mu(X) = 0, \quad \partial_\mu \Theta_{\text{loc}}^{\mu\nu}(X) = 0, \quad \text{with} \quad (60)$$

$$J^\mu(X) = \sum_a e_a \int \frac{d^4p}{(2\pi)^4} p^\mu f_a(X, p) A_a(X, p), \quad (61)$$

$$\begin{aligned} \Theta_{\text{loc}}^{\mu\nu}(X) &= \sum_a \underbrace{\int \frac{d^4p}{(2\pi)^4} v^\mu p^\nu f_a(X, p) A_a(X, p)}_{\text{sum of single particle terms}} \\ &\quad + g^{\mu\nu} (\mathcal{E}_{\text{loc}}^{\text{int}}(X) - \mathcal{E}_{\text{loc}}^{\text{pot}}(X)), \end{aligned} \quad (62)$$

here written in terms of the product of phase-space occupation and spectral functions $f_a(X, p)A_a(X, p) = (\mp i)G_a^{-+}(X, p)$, are exact consequences of the equations of motion. In order to preserve this exact conserving property, two conditions have to be met. First, the original KB equations should be based on a Φ -derivable approximation scheme that guarantees that the KB equations themselves are conserving [38, 18]. The second condition is that the gradient expansion has to be done systematically, whereby it is important that no further approximations are applied that violate the balance between the different first-order gradient terms.

Indeed, all gradient terms residing in the Poisson brackets and in the memory collision term cancel each other for the conserved currents such that the original Noether expression (61) remains conserved. This implies the compensation of drag-flow terms by all the other gradient terms (back-flow and memory flow), cf. the discussion given in ref. [18]. For the energy-momentum tensor the gradient terms result into the divergence of the difference between interaction energy density and single-particle potential energy density, cf. (62). Thereby $\mathcal{E}_{\text{loc}}^{\text{int}}(X)$ and $\mathcal{E}_{\text{loc}}^{\text{pot}}(X)$ are obtained from the same Φ -functional in the local approximation as the self-energies driving the equations of motion (5) and (9). The so obtained energy-momentum tensor is general and applies to any local coupling scheme. The energy component Θ_{loc}^{00} has a simple interpretation. The first term determines the single-particle energy, which consists of the kinetic and single-particle potential energy parts. Evidently this part by itself is not conserved⁵. Rather its potential energy part is compensated by the last term, i.e. $\mathcal{E}_{\text{loc}}^{\text{pot}}(X)$, such that finally the total kinetic plus interaction energy survive.

A typical example for the imbalance of gradient terms is the case, where one neglects the second Poisson bracket term in (10). This implies that drag-flow effects contained in the first Poisson bracket remain uncompensated. Also possible memory effects C_{mem} in the collision term should not be omitted. Otherwise the Poisson brackets $\{\text{Re}\Sigma_a^R, iG_a^{-+}\} + \{i\Sigma_a^{-+}, \text{Re}G_a^R\}$ remain uncompensated and, as a consequence, the conservation laws are again violated already in zero-order gradients.

A less evident example is the modification of the gradient terms after the formal gradient expansion, as it has been suggested by Botermans and Malfliet [10], see also [18]. There one simplifies those self-energy terms that are involved in the Poisson brackets $\{\text{Re}\Sigma_a^R, iG_a^{-+}\} + \{i\Sigma_a^{-+}, \text{Re}G_a^R\}$, employing quasi-equilibrium relations. This modification implies deviations at second-order gradients only⁶, which is quite acceptable from the formal

⁵Contrary to the constructions given in ref. [52].

⁶This freedom of choice is due to the fact that various redundant combinations of the KB equations lead to non-redundant equations after gradient approximation due to the asymmetric treatment of sums and differences of the KB equations and their adjoint ones in the gradient approximation. The so called mass-shell equation indeed agrees

$$-i\Sigma(x, y) = \text{[Hartree diagram]} + \sum_{n=2}^{\infty} \text{[RPA diagram with } n \text{ dashed lines]}, \quad (64)$$

which is just the finite range analog of the Fermi-liquid example (34), now for the particle-particle resummation channel. Here n counts the number of interaction (dashed) lines representing the two-body potential $V(x_i - x_k)$. The first terms in both expressions are the usual Hartree terms. The remaining sum leads to a conserving T -matrix type of approximation for the self-energies (64), which, e.g., provides thermodynamically consistent description of the nuclear matter [53–55]. In the dilute limit it expresses the self-energies through the vacuum scattering T -matrix [56, 57, 15]. In this limit it provides a collision term given by vacuum scattering cross sections and at the same time the gradient terms account for the appropriate virial corrections. The latter indirectly depend on the energy variations of the corresponding phase shifts, which give rise to delay time effects [58, 15] and the corresponding changes of the underlying equation of state (energy-momentum tensor) [59, 61–63]. Furthermore, the s -channel bosonization of the interactions in the particle-hole channel, cf. ref. [18], leads to the RPA-approximation. Further applications and considerations of the quantum transport equations will be discussed in a forthcoming paper.

A case that still requires a separate treatment is that of derivative coupling of relativistic fields, as e.g., in the case of the pion-nucleon interaction. The reason is that derivative couplings produce extra terms in the currents and the energy-momentum tensor, which require special treatment.

Besides all this success at the one-particle expectation value level, one has to keep in mind that partial Dyson resummations still may violate the symmetries at the two-body correlator level and beyond. In particular, it means that the corresponding Ward-Takahashi identities are not necessarily fulfilled within the Φ -derivable Dyson resummation scheme. On the other side the Φ -derivable scheme provides the tools to construct the driving terms and kernels of the corresponding higher order vertex equations (Bethe-Salpeter equations, etc.) which precisely recover the conservation laws at the correlator level [37, 38, 64, 65]. So far such equations, however, could mostly be solved in drastically simplified cases (e.g., by RPA-type resummation). A particular challenge represents the inclusion of vector or gauge bosons into a self-consistent Dyson scheme beyond the mean-field level, i.e. at the propagator level, since partial Dyson resummations violate the four-dimensional transversality of the propagators. A practical way out of this difficulty has recently been suggested in refs. [23, 64]. A further virtue of the Φ -derivable scheme is that it apparently permits a renormalization of the non-perturbative self-consistent self-energies with temperature- and density-independent counter terms [64].

ACKNOWLEDGMENTS

We are grateful to G. Baym, P. Danielewicz, H. Feldmeier, B. Friman, H. van Hees, C. Greiner, E.E. Kolomeitsev and S. Leupold for fruitful discussions on various aspects of this research. Two of us (Y.B.I. and D.N.V.) highly appreciate the hospitality and support rendered to us at Gesellschaft für Schwerionenforschung. This work has been supported in part by DFG (project 436 Rus 113/558/0). Y.B.I and D.N.V. were partially supported by RFBR grant NNIO-00-02-04012. Y.B.I. was also partially supported by RFBR grant 00-15-96590.

APPENDIX A

A.1. CONTOUR MATRIX NOTATION

In calculations that apply the Wigner transformations, it is necessary to decompose the full contour into its two branches—the *time-ordered* and *anti-time-ordered* branches. One then has to distinguish between the physical space-time coordinates x, \dots and the corresponding contour coordinates $x^{\mathcal{C}}$ which for a given x take two values $x^- = (x_\mu^-)$ and $x^+ = (x_\mu^+)$ ($\mu \in \{0, 1, 2, 3\}$) on the two branches of the contour (see figure 1). Closed real-time contour integrations can then be decomposed as

$$\begin{aligned} \int_{\mathcal{C}} dx^{\mathcal{C}} \dots &= \int_{t_0}^{\infty} dx^- \dots + \int_{\infty}^{t_0} dx^+ \dots \\ &= \int_{t_0}^{\infty} dx^- \dots - \int_{t_0}^{\infty} dx^+ \dots, \end{aligned} \quad (\text{A.1})$$

where only the time limits are explicitly given. The extra minus sign of the anti-time-ordered branch can conveniently be formulated by a $\{-+\}$ “metric” with the metric tensor in $\{-+\}$ indices

$$(\sigma^{ij}) = (\sigma_{ij}) = \begin{pmatrix} 1 & 0 \\ 0 & -1 \end{pmatrix} \quad (\text{A.2})$$

which provides a proper matrix algebra for multi-point functions on the contour with “co”- and “contra”-contour values. Thus, for any two-point function F , the contour values are defined as

$$\begin{aligned} F^{ij}(x, y) &:= F(x^i, y^j), \quad i, j \in \{-, +\}, \quad \text{with} \\ F_i^j(x, y) &:= \sigma_{ik} F^{kj}(x, y), \quad F_j^i(x, y) := F^{ik}(x, y) \sigma_{ki} \\ F_{ij}(x, y) &:= \sigma_{ik} \sigma_{jl} F^{kl}(x, y), \quad \sigma_i^k = \delta_{ik} \end{aligned} \quad (\text{A.3})$$

on the different branches of the contour. Here summation over repeated indices is implied. Then contour folding of contour two-point functions, e.g. in Dyson equations, simply becomes

$$\begin{aligned} H(x^i, y^k) = H^{ik}(x, y) &= \int_{\mathcal{C}} dz^{\mathcal{C}} F(x^i, z^{\mathcal{C}}) G(z^{\mathcal{C}}, y^k) \\ &= \int dz F_j^i(x, z) G^{jk}(z, y) \end{aligned} \quad (\text{A.4})$$

in the matrix notation.

For any multi-point function the external point x_{max} , which has the largest physical time, can be placed on either branch of the contour without changing the value, since the contour-time evolution from x_{max}^- to x_{max}^+ provides unity. Therefore, one-point functions have the same value on both sides of the contour.

Due to the change of operator ordering, genuine multi-point functions are, in general, discontinuous, when two contour coordinates become identical. In particular, two-point functions like $iF(x, y) = \langle \mathcal{T}_{\mathcal{C}} \hat{A}(x) \hat{B}(y) \rangle$ become

$$\begin{aligned} iF(x, y) &= \begin{pmatrix} iF^{--}(x, y) & iF^{-+}(x, y) \\ iF^{+-}(x, y) & iF^{++}(x, y) \end{pmatrix} \\ &= \begin{pmatrix} \langle \mathcal{T} \hat{A}(x) \hat{B}(y) \rangle & \mp \langle \hat{B}(y) \hat{A}(x) \rangle \\ \langle \hat{A}(x) \hat{B}(y) \rangle & \langle \mathcal{T}^{-1} \hat{A}(x) \hat{B}(y) \rangle \end{pmatrix}, \end{aligned} \quad (\text{A.5})$$

where \mathcal{T} and \mathcal{T}^{-1} are the usual time and anti-time ordering operators. Since there are altogether only two possible orderings of the two operators, in fact given by the Wightman functions F^{-+} and F^{+-} , which are both continuous, not all four components of F are independent. Eq. (A.5) implies the following relations between non-equilibrium and usual retarded and advanced functions

$$\begin{aligned} F^R(x, y) &:= \Theta(x_0 - y_0) (F^{+-}(x, y) - F^{-+}(x, y)), \\ &= F^{--}(x, y) - F^{-+}(x, y) = F^{+-}(x, y) - F^{++}(x, y) \\ F^A(x, y) &:= -\Theta(y_0 - x_0) (F^{+-}(x, y) - F^{-+}(x, y)) \\ &= F^{--}(x, y) - F^{+-}(x, y) = F^{-+}(x, y) - F^{++}(x, y), \end{aligned} \quad (\text{A.6})$$

where $\Theta(x_0 - y_0)$ is the step function of the time difference. The rules for the co-contour functions F_{--} etc. follow from Eq. (A.3).

Discontinuities of a two-point function may cause problems for differentiations, in particular, since they often occur simultaneously in products of

two or more two-point functions. The proper procedure is, first, with the help of Eq. (A.5) to represent the discontinuous parts in F^{--} and F^{++} by the continuous F^{-+} and F^{+-} times Θ -functions, then to combine all discontinuities, e.g. with respect to $x_0 - y_0$, into a single term proportional to $\Theta(x_0 - y_0)$, and finally to apply the differentiations. One can easily check that in the following particularly relevant cases

$$\int_{\mathcal{C}} dz (F(x^i, z)G(z, x^j) - G(x^i, z)F(z, x^j)), \quad (\text{A.7})$$

$$\frac{\partial}{\partial x_\mu} \int_{\mathcal{C}} dz (F(x^i, z)G(z, x^j) + G(x^i, z)F(z, x^j)), \quad (\text{A.8})$$

$$\left[\left(\frac{\partial}{\partial x_\mu} - \frac{\partial}{\partial y_\mu} \right) \int_{\mathcal{C}} dz (F(x^i, z)G(z, y^j) - G(x^i, z)F(z, y^j)) \right]_{x=y} \quad (\text{A.9})$$

all discontinuities exactly cancel. Thereby, these values are independent of the placement of x^i and x^j on the contour, i.e. the values are only functions of the physical coordinate x .

For such two point functions complex conjugation implies

$$\begin{aligned} (iF^{-+}(x, y))^* &= iF^{-+}(y, x) &\Rightarrow & iF^{-+}(X, p) = \text{real}, \\ (iF^{+-}(x, y))^* &= iF^{+-}(y, x) &\Rightarrow & iF^{+-}(X, p) = \text{real}, \\ (iF^{--}(x, y))^* &= iF^{++}(y, x) &\Rightarrow & (iF^{--}(X, p))^* = iF^{++}(X, p), \\ (F^R(x, y))^* &= F^A(y, x) &\Rightarrow & (F^R(X, p))^* = F^A(X, p), \end{aligned} \quad (\text{A.10})$$

where the right parts specify the corresponding properties in the Wigner representation. Diagrammatically these rules imply the simultaneous swapping of all $+$ vertices into $-$ vertices and vice versa together with reversing the line arrow-sense of all propagator lines in the diagram.

REFERENCES

1. J. Schwinger, *J. Math. Phys.* **2** (1961), 407.
2. L. P. Kadanoff and G. Baym, “Quantum Statistical Mechanics”, Benjamin, NY, 1962.
3. L. P. Keldysh, *ZhETF* **47** (1964), 1515; Engl. transl., *Sov. Phys. JETP* **20** (1965), 1018.
4. E. M. Lifshiz and L. P. Pitaevskii, “Physical Kinetics”, Pergamon press, 1981.
5. N. P. Landsman and Ch. G. van Weert, *Phys. Rep.* **145** (1987), 141.
6. J. P. Blaizot and E. Iancu, hep-ph/0101103.
7. P. Danielewicz, *Ann. Phys. (N.Y.)* **152** (1984), 239, and 305.
8. P. Danielewicz, *Ann. Phys. (N.Y.)* **197** (1990), 154.
9. M. Tohyama, *Phys. Rev. C* **86** (1987), 187.
10. W. Botermans and R. Malfliet, *Phys. Rep.* **198** (1990), 115.

11. A. B. Migdal, E. E. Saperstein, M. A. Troitsky and D. N. Voskresensky, *Phys. Rep.* **192** (1990), 179.
12. D. N. Voskresensky, *Nucl. Phys. A* **555** (1993), 293.
13. P.A. Henning, *Phys. Rep. C* **253** (1995), 235.
14. J. Knoll and D. N. Voskresensky, *Phys. Lett. B* **351** (1995), 43;
J. Knoll and D. N. Voskresensky, *Ann. Phys. (N.Y.)* **249** (1996), 532.
15. Yu. B. Ivanov, J. Knoll, and D. N. Voskresensky, *Nucl. Phys. A* **657** (1999), 413.
16. P. Bozek, *Phys. Rev. C* **59** (1999), 2619.
17. J. Knoll, *Prog. Part. Nucl. Phys.* **42** (1999), 177.
18. Yu. B. Ivanov, J. Knoll, and D. N. Voskresensky, *Nucl. Phys. A* **672** (2000), 313.
19. W. Cassing and S. Juchem, *Nucl. Phys. A* **665** (2000), 377; **672** (2000), 417.
20. S. Leupold, *Nucl. Phys. A* **672** (2000), 475.
21. M. Effenberger, U. Mosel, *Phys. Rev. C* **60** (1999), 51901.
22. Yu. B. Ivanov, J. Knoll, H. van Hees and D. N. Voskresensky, e-Print Archive: nucl-th/0005075; *Yad. Fiz.* **64** (2001).
23. H. van Hees, and J. Knoll, *Nucl. Phys. A* **A683** (2001), 369.
24. D. N. Voskresensky and A. V. Senatorov, *Yad. Fiz.* **45** (1987), 657; Engl. transl., *Sov. J. Nucl. Phys.* **45** (1987), 414.
25. W. Keil, *Phys. Rev. D* **38** (1988), 152.
26. E. Calzetta and B. L. Hu, *Phys. Rev. D* **37** (1988), 2878.
27. M. Månson, and A. Sjölander, *Phys. Rev. B* **11** (1975), 4639.
28. V. Korenman, *Ann. Phys. (N.Y.)* **39** (1966), 72.
29. B. Bezzerides and D. F. DuBois, *Ann. Phys. (N.Y.)* **70** (1972), 10.
30. W. D. Kraeft, D. Kremp, W. Ebeling and G. Röpke, "Quantum Statistics of Charged Particle Systems", Akademie-Verlag, Berlin, 1986.
31. J. W. Serene and D. Rainer, *Phys. Rep.* **101** (1983), 221.
32. K. Chou, Z. Su, B. Hao and L. Yu, *Phys. Rep.* **118** (1985), 1.
33. J. Rammer and H. Smith, *Rev. Mod. Phys.* **58** (1986), 323.
34. R. Fauser, *Nucl. Phys. A* **606** (1996), 479.
35. V. Spicka and P. Lipavsky, *Phys. Rev. Lett.* **73** (1994), 3439; *Phys. Rev. B* **52** (1995), 14615.
36. P. Nozières, and E. Abrahams, *Phys. Rev. B* **10** (1974), 4932;
S. Abraham - Ibrahim, B. Caroli, C. Cardì, and B. Roulet, *Phys. Rev. B* **18** (1978), 6702.
37. G. Baym and L. P. Kadanoff, *Phys. Rev.* **124** (1961), 287.
38. G. Baym, *Phys. Rev.* **127** (1962), 1391.
39. J. M. Luttinger and J. C. Ward, *Phys. Rev.* **118** (1960), 1417.
40. A. A. Abrikosov, L. P. Gorkov, I. E. Dzyaloshinski, "Methods of Quantum Field Theory in Statistical Physics", Dover Pub., INC. N.Y., 1975.
41. J. M. Cornwall, R. Jackiw and E. Tomboulis, *Phys. Rev. D* **10** (1974), 2428.
42. P. Lipavsky, V. Spicka and B. Velicky, *Phys. Rev. B* **34** (1986), 6933.
43. M. Bonitz, "Quantum Kinetic Theory", Teubner, Stuttgart/Leipzig, 1998.
44. Th. Bornath, D. Kremp, W. D. Kräft, and M. Schlanges, *Phys. Rev. E* **54** (1996), 3274.
45. M. Schönhofen, M. Cubero, B. Friman, W. Nörenberg and Gy. Wolf, *Nucl. Phys. A* **572** (1994), 112.
46. S. Jeon and L.G. Yaffe, *Phys. Rev. D* **53** (1996), 5799.

47. D. N. Voskresensky, D. Blaschke, G. Röpke and H. Schulz, *Int. Mod. Phys. J. E* **4** (1995), 1.
48. P. Danielewicz and G. Bertsch, *Nucl. Phys. A* **533** (1991), 712.
49. E. Riedel, *Z. Phys. A* **210** (1968), 403.
50. G. M. Carneiro and C. J. Pethick, *Phys. Rev. B* **11** (1975), 1106.
51. G. Baym and C. Pethick, “Landau Fermi–Liquid Theory”, John Wiley and Sons, INC, N.Y., 1991.
52. W. Cassing and S. Juchem, *Nucl. Phys. A* **677** (2000), 445.
53. P. Bożek and P. Czerski, nucl-th/0102020; P. Bożek, *Phys. Rev. C* **59** (1999), 2619; *Nucl. Phys. A* **657** (1999), 187.
54. W. H. Dickhoff, *Phys. Rev. C* **58** (1998), 2807; W. H. Dickhoff *et al.*, *Phys. Rev. C* **60** (1999), 4319.
55. Y. Dewulf, D. Van Neck and M. Waroquier, nucl-th/0012022.
56. W. Lenz, *Z. Phys.* **56** (1929), 778.
57. C. B. Dover, J. Hüfner and R. H. Lemmer, *Ann. Phys. (N.Y.)* **66** (1971), 248.
58. P. Danielewicz and S. Pratt, *Phys. Rev. C* **53** (1996), 249.
59. E. Beth, G. E. Uhlenbeck, *Physica* **4** (1937), 915.
60. K. Huang, “Statistical Mechanics”, Wiley, New York (1963).
61. R. Dashen, S. Ma, H. J. Bernstein, *Phys. Rev.* **187** (1969), 345.
62. A. Z. Mekjian, *Phys. Rev. C* **17** (1978), 1051.
63. R. Venugopalan and M. Prakash, *Nucl. Phys. A* **456** (1992), 718.
64. H. van Hees, Ph-D thesis, Tu-Darmstadt, Germany, Landes und Hochschulbibliothek, Oct. 2000, <http://elib.tu-darmstadt.de/diss/000082/>, to be published in parts.
65. H. van Hees and J. Knoll, to be published.